2020-07-28

Calculation of electrical conductivity of self-sensing carbon nanotube composites

Fang, Y

10.1016/j.compositesb.2020.108314
Composites Part B: Engineering
Elsevier BV

Composites Part B: Engineering
Received 26 May 2020, Revised 25 June 2020, Accepted 20 July 2020, Available online 28 July 2020
https://doi.org/10.1016/j.compositesb.2020.108314

Calculation of electrical conductivity of self-sensing carbon nanotube composites

Yuan Fang[1], Long-Yuan Li[2], Sung-Hwan Jang[3]

1) Guangdong Provincial Key Laboratory of Durability for Maine Civil Engineering, Shenzhen University, Shenzhen 518060, P R China (yuanfang@szu.edu.cn)
2) School of Engineering, Computing and Mathematics, University of Plymouth, Plymouth, Devon PL7 8AA, UK (long-yuan.li@plymouth.ac.uk)
3) School of Engineering, Hanyang University ERICA, Ansan, Gyeonggi-do 15588, South Korea (sj2527@hanyang.ac.kr)

Abstract – This paper presents an analytical study on the electrical conductivity of composites whose constituted materials have distinct electrical properties. The present study investigates the effect of the aspect ratio of inclusions on the effective electrical conductivity of composites. Formulations are derived for determining the percolation threshold and calculating the electrical conductivity of composites with considering aspect ratio effect. The validation of the present model is also provided by using available experimental data. The present analytical model can be applied to predict the electrical behaviour of carbon-nanotube fibre reinforced polymer composites.

Keywords: Carbon nanotubes; electrical conductivity; composites; percolation threshold; modelling.

1. Introduction

Carbon nanotubes (CNTs) are the cylinders made of carbon with diameters in nanoscale. CNTs can be single-walled or multi-walled; the latter consist of several concentrically-interlinked nanotubes. Owing to their molecularly perfect, CNTs are free of property-degrading flaws in their structure and thus have unique thermal, electrical and mechanical properties. These features make CNTs highly attractive for numerous applications such as electronics, optics, and smart composite materials [1].

The piezoresistive behaviour of the composites formed by polymers with embedded CNTs can be used to make electromechanical and/or electrothermal sensors [2,3]. This is because when a CNTs-reinforced polymer composite is subjected to externally applied thermal or mechanical loading, the percolated CNTs network is disrupted, resulting in a change in resistivity. The variation in resistivity under a load is attributed to the variation in contact configurations and channelling distances among the contacting CNTs upon nanocomposite deformation. The

strain sensing ability of CNTs-composites has been considered to be a key requirement for the development of smart materials and structural health monitoring techniques. One of the fundamental issues in developing such smart sensors made from CNTs-composites is to identify how the electrical conductivity or resistivity of the formed composite varies with the amount and arrangement of CNTs in the composite and how the microstructure of the composite alters in response to the change of surrounding environment conditions. Numerous studies have been conducted on the relationship between the thermal and/or electrical conductivity and the volume fraction of CNTs into polymeric composites. For example, Ni et al. [4] investigated experimentally the shape memory effect and dynamic mechanical properties of CNTs/shape-memory-polymer (SMP) nanocomposites. It was found that storage elastic modulus was improved noticeably with increased weight fraction of CNTs and the recovery stress of the CNTs/SMP nanocomposites with 3.3% wt fraction of CNTs can reach almost twice of that in pure SMP. Pham et al. [5] reported the development of conductive CNTs-filled polymer composite films as strain sensors with tailored sensitivity. A semi-empirical model was also proposed to show the relationship between the volume fraction of CNTs and the sensitivity of the composite films. Dastgerdi et al. [6] developed a micro-mechanical model to take into account the waviness effect of CNTs on the effective stiffness of CNTs/SMP composites. It was found that the waviness distribution has a significant influence on the prediction of the composite stiffness. Lu et al. [7] examined the infrared light-induced shape memory effect and thermomechanical properties of SMP nanocomposites incorporated with CNTs and boron nitride. It was found that the combined use of CNTs and boron nitride resulted in higher glass transition temperature and better thermomechanical strengths. Jomaa et al. [8] investigated the elastic, electrical and electromechanical properties of grafted-CNTs/ polyurethane nanocomposites and demonstrated how grafting polymer onto CNTs can improve the physical properties of polyurethane nanocomposites. Arani et al. [9] and Kolahchi et al. [10] presented the wave propagation analysis of CNTs reinforced nanocomposite polymeric piezoelectric micro plates and piezoelectric sandwich plates. The effects of various parameters including geometric constants, viscoelastic foundation, structural damping coefficient, applied voltage, volume fraction and distribution type of CNTs, temperature and magnetic field on the analysis and control of the wave propagation in the smart nanocomposite structures were examined. Aghdam et al. [11] investigated the thermal conductivity of SMP nanocomposites containing CNTs, in which the effects of volume fraction, diameter, cross-section shape, arrangement type and waviness factors of CNTs as well as interfacial thermal resistance on the axial and transverse thermal conductivities of aligned CNTs/SMP nanocomposites were examined. The results showed that the alignment of CNTs into SMP nanocomposites along the thermal loading can be an efficient way to dissipate the heat. Xia et al. [12] investigated the electrical conductivity and dielectric permittivity of highly aligned graphene-based nanocomposites. Simulations using Monte Carlo method were carried out by Fang et al. [13] to calculate the electrical conductivity of graphene nanoplatelet polymer composites, Spanos et al. [14] to estimate the physical properties of nanocomposites, and Liu et al. [15] to determine the radiation-induced conductivity change of carbon nanotube filled polymers. The abovementioned works show there are significant achievements in the application of CNTs for developing smart sensors. However, most of these works are the experimental-based studies and there is lack of prediction models which can be used to directly estimate the thermal,

electrical or mechanical properties of the CNTs/polymer nanocomposites based on the volume fractions and properties of CNTs and polymer materials themselves.

In literature there have been a large number of studies on the effective electrical conductivity of two-phase composite materials, although they were not directly addressed on the CNTs/polymer composite materials. The early work can date back to 1930s, when an empirical model was developed by Bruggeman [16], in which the electrical conductivity of the two-component composite is expressed in terms of the electrical conductivities and volume fractions of the two constituted components. The Bruggeman model predicts the percolation effect but with a fixed percolation threshold 0.33, which largely restricts its application. Attempts have been made by many researchers to modify Bruggeman model by using more empirical parameters in the expression to adapt various variations caused by the shape of inclusions and interaction between inclusions and medium [17,18,19]. A detailed literature review on the development of the empirical models can be found elsewhere [19,20].

In this paper a prediction model is presented for the electrical conductivity of CNTs reinforced polymer composites. The model is developed based on the previously experimental study [21] on self-sensing CNTs-composites. The aim of the model is to connect the percolation theory with the volume fraction of CNTs with considering the effects of the aspect ratio of CNTs on the effective electrical conductivity of the CNTs reinforced polymer composites. The main novelty of the present work is the percolation threshold that is derived based on the aspect ratio of the CNTs and the percolation effect is considered both before and after the percolation. In addition all parameters used in the model have clear physical meaning and thus are convenient to determine.

2. Calculation of electrical conductivity in composite materials

The electrical resistance of an object is a measure of its opposition to the flow of electric current. It can be determined simply by measuring the voltage across the object and the current through the object, and then using the following well-known Ohm's law

$$V = RI \tag{1}$$

where V is the voltage across the object, R is the electrical resistance of the object, and I is the current through the object. In order to eliminate the size effect of the object Eq.(1) is rewritten as follows,

$$\frac{V}{L} = \left(\frac{RA}{L}\right)\frac{I}{A} = \frac{1}{\sigma}\frac{I}{A} \tag{2}$$

where L is the length of the object, A is the cross-sectional area of the object, V/L represents the magnitude of the electric field, I/A represents the current density, RA/L is the electrical resistivity, and $\sigma=L/(RA)$ is the electrical conductivity and has the SI units of siemens per metre (S/m).

Consider a composite material made from two components. The bulk electrical conductivity of the composite material is dependent not only on the electrical conductivities and volume fractions of the two constituted materials but also on the manner how these two components

are mixed and configurated in the composite. Without loss of generality, we assume one component is the homogeneous medium and the other component represents a finite number of inclusions. Let σ_e be the effective electrical conductivity of the composite; σ_i and V_i be the electrical conductivity and volume fraction of the inclusions; σ_m and V_m be the electrical conductivity and volume fraction of the medium, respectively. Many approaches can be used to calculate the effective electrical conductivity of the composite. One is the analytical approach developed based on simplified models [22,23,24]; the other is the numerical simulation based on two-phase models [24,25,26]. Fig.1a and Fig.1c show the parallel and series models, respectively; whereas Fig.1b can be treated as the spherical model if the inclusions are assumed to be embedded in the medium. In Fig.1 the materials of inclusions and medium in the representative volume element (RVE) of the composite are represented by using two different colours. The parallel, series and spherical models are commonly used for the prediction of σ_e. According to the theoretical formula of the parallel, spherical and series models [27,28,29,30], the effective electrical conductivity of the composite can be estimated as follows,

(1) Parallel model:

$$\sigma_e = \frac{\sigma_m V_m}{V_i+V_m} + \frac{\sigma_i V_i}{V_i+V_m} \tag{3}$$

(2) Spherical model:

$$\sigma_e = \frac{2V_m\sigma_m^2+(3V_i+V_m)\sigma_i\sigma_m}{(3V_i+2V_m)\sigma_m+V_m\sigma_i} \tag{4}$$

$$\sigma_e = \frac{2V_i\sigma_i^2+(3V_m+V_i)\sigma_i\sigma_m}{(3V_m+2V_i)\sigma_i+V_i\sigma_m} \tag{5}$$

(3) Series model:

$$\sigma_e = \frac{(V_i+V_m)\sigma_m\sigma_i}{V_i\sigma_m+V_m\sigma_i} \tag{6}$$

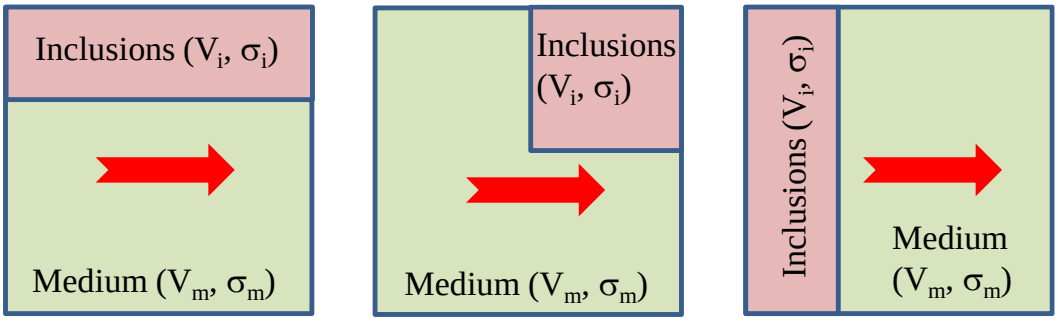

(a) (b) (c)

Figure 1. Analytical models for calculation of electrical conductivity in a two-component composite material. (a) Parallel model. (b) Spherical model. (c) Series model.

Theoretically, the parallel model gives the upper bound of σ_e and the series model gives the lower bound of σ_e. There are two formulas in the spherical model. One is obtained by assuming the medium as the outer layer of the sphere and the other is obtained by assuming the inclusions as the outer layer of the sphere. The former is more suitable for $V_i<V_m$, whereas the latter is more suitable for $V_i>V_m$. Thus, a combination of them shown below can also be used,

$$\sigma_e = \frac{2V_m\sigma_m^2+(3V_i+V_m)\sigma_i\sigma_m}{(3V_i+2V_m)\sigma_m+V_m\sigma_i}\left(1-\frac{V_i}{V_m+V_i}\right)+\frac{2V_i\sigma_i^2+(3V_m+V_i)\sigma_i\sigma_m}{(3V_m+2V_i)\sigma_i+V_i\sigma_m}\left(\frac{V_i}{V_m+V_i}\right) \quad (7)$$

Fig.2 shows the comparison of the effective electrical conductivities σ_e of the composite material calculated using Eqs.(3)-(7) for two cases; one is for $\sigma_i>>\sigma_m$ ($\sigma_i=50\sigma_m$) and the other is for $\sigma_i<<\sigma_m$ ($\sigma_m=50\sigma_i$). It can be seen from the figure that the curves given by the spherical models using Eqs.(4) and (5) are closer to those given by the series and parallel models, respectively; whereas the curve given by the combined spherical model using Eq.(7) is between them, indicating that the combination of the two spherical models could be more appropriate and realistic. The concept of using the combined spherical model is because in a real composite neither the inclusions nor the medium would be perfectly covered by the medium or by the inclusions. In other words, the inclusions and medium in the composite should have equal opportunity to give their function and they should be able to be swapped each other in their predicted equation. In literature similar modifications on the spherical model have been also suggested but with different formulas [16,17,18].

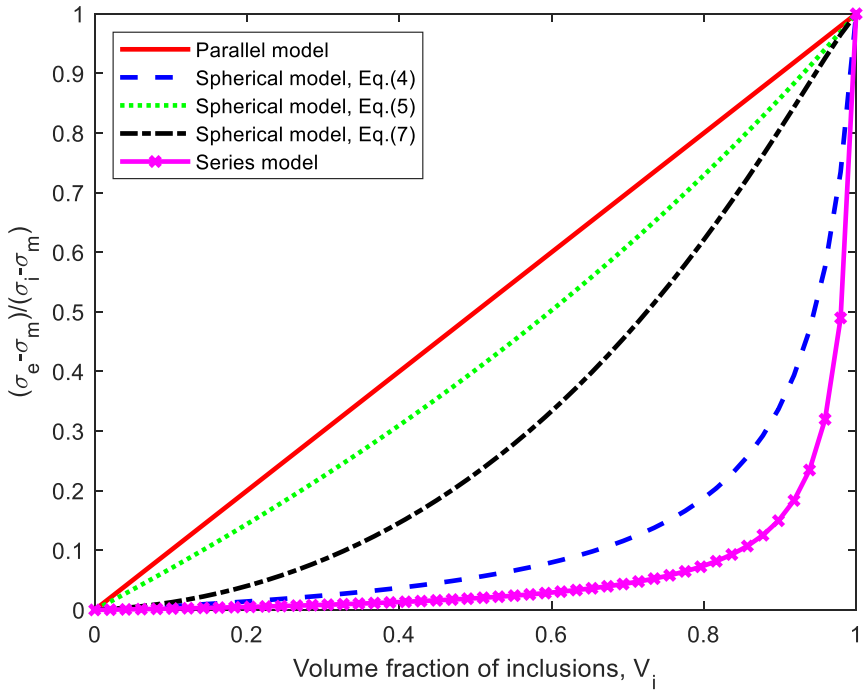

(a)

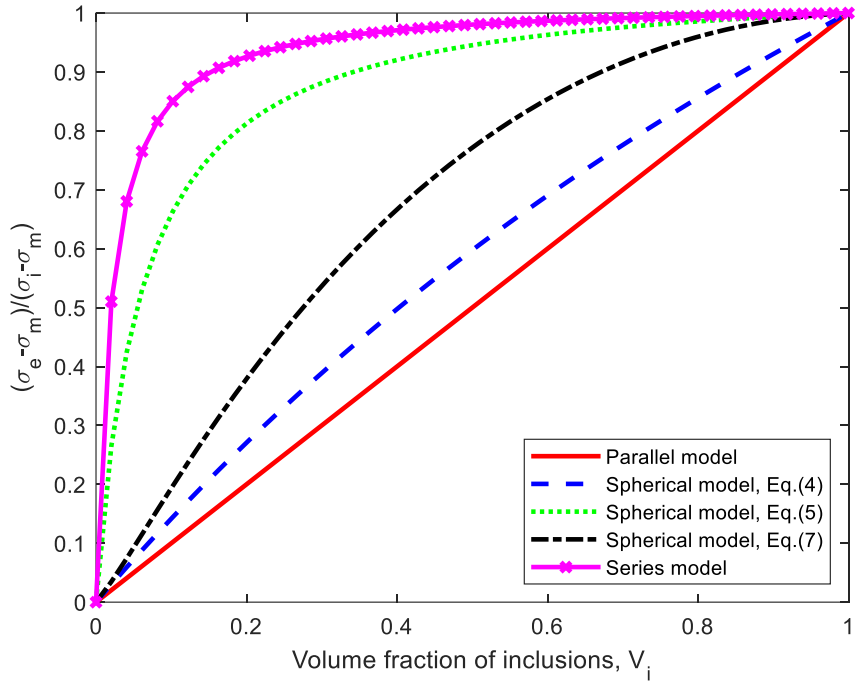

(b)

Figure 2. Predicted effective electrical conductivity of two-component composite from different models for cases of (a) $\sigma_i=50\sigma_m$ and (b) $\sigma_m=50\sigma_i$.

3. Aspect ratio effect of inclusions on electrical conductivity of composites

It should be noted that Eqs.(4) and (5) are derived based on the assumption that the inclusions are the spherical shape and they are uniformly distributed in the medium. In many applications, however, the inclusions may not be spherical particles, but have large aspect ratio. One typical example for this is the self-sensors of CNTs reinforced epoxy composites [21,31,32,33,34], in which the epoxy acts as a very low conductive medium, whereas the high conductive CNTs of needle/fibre shape are the inclusions. The electrical conductivity of the CNTs-reinforced epoxy composite depends on not only the volume fraction of the CNTs embedded in the composite but also the aspect ratio of the CNTs employed, particularly when the volume fraction of the inclusions is small.

In order to examine the effect of the aspect ratio of CNTs on the electrical conductivity of the CNTs-reinforced polymer composite, herein we assume the CNTs themselves are isotropic and uniformly dispersed in the composite when they are mixed with polymer. Consider a unit volume of RVE of the composite material. Assume the accumulated CNTs are equally distributed in x-, y-, and z-axial directions within the RVE and can be approximately represented by the configuration of three-prisms shown in Fig.3a, in which the dimensions of the prism are λa x a x a (see Fig.3c) where λ is the aspect ratio of the CNTs and a is a constant that depends on the CNTs volume fraction in the composite. It is obvious that if $\lambda=1$ then the

three prisms reduce to a cube of size length *a*, which is similar to the spherical model shown in Fig.1b.

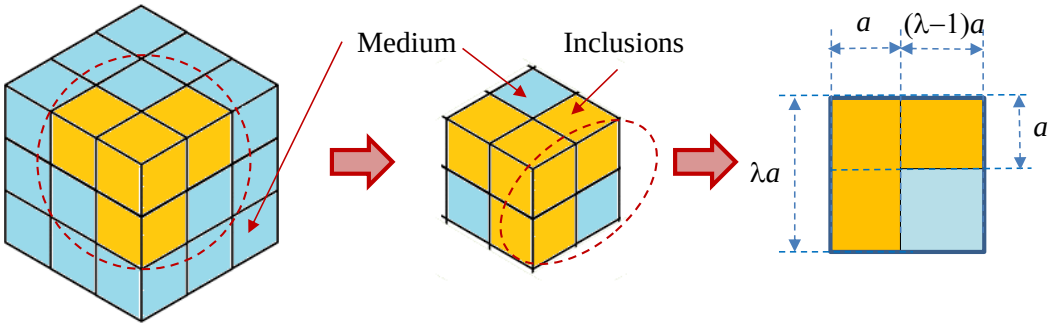

Figure 3. Schematic of fibre-reinforced composite material (blue and yellow represent medium and inclusions). (a) A unit volume cube of RVE of composite. (b) Sub-domain involving inclusions. (c) Side view and dimensions of sub-domain.

For a given aspect ratio λ, the constant *a* can be determined based on the volume fraction of CNTs in the composite. According to the configuration shown in Fig.3a, if $\lambda a < 1$, we have

Case 1: $\lambda a < 1$

$$V_i = 3\lambda a^3 - 2a^3 = (3\lambda - 2)a^3 \tag{8}$$

$$V_{m1} = (\lambda a)^3 - (3\lambda - 2)a^3 = (\lambda^3 - 3\lambda + 2)a^3 \tag{9}$$

$$V_{m2} = 1 - (\lambda a)^3 \tag{10}$$

where V_i is the volume of CNTs in the sub-domain which equals to the volume fraction of CNTs in the composite, V_{m1} is the volume of the medium in the sub-domain shown in Fig.3b, V_{m2} is the volume of the medium in the unit volume of cube subtract the sub-domain. $V_m=V_{m1}+V_{m2}$ is the volume fraction of the medium in the composite. It is obvious that for a given value of λ, *a* increases with the volume fraction V_i of CNTs. Thus, for a large value of λ it is possible that $\lambda a = 1$ (that is, the CNTs becomes connective from one side to the other side in the unite volume of RVE). In this case, we have

Case 2: $\lambda a = 1$

$$V_i = 3a^2 - 2a^3 = (3 - 2a)a^2 \tag{11}$$

$$V_{m1} = 1 - (3 - 2a)a^2 \tag{12}$$

$$V_{m2} = 0 \tag{13}$$

The calculation of the effective electrical conductivity of the RVE in Case 1 can be divided into two steps. The first step is to calculate the effective electrical conductivity, $\sigma_e^{(1)}$, of the sub-domain shown in Fig.3b, in which the two components are the CNTs with volume V_i and conductivity σ_i and the medium with volume V_{m1} and conductivity σ_m. Since the inclusions are connective in the sub-domain $\sigma_e^{(1)}$ can be calculated using Eq.(5) as follows,

$$\sigma_e^{(1)} = \frac{2V_i\sigma_i^2+(3V_{m1}+V_i)\sigma_i\sigma_m}{(3V_{m1}+2V_i)\sigma_i+V_i\sigma_m} \tag{14}$$

The second step is to calculate the effective electrical conductivity of the RVE shown in Fig.3a, in which the sub-domain is completely covered by the medium and the corresponding two components are the sub-domain component with volume $V_i^*=V_i+V_{m1}$ and conductivity $\sigma_i^*= \sigma_e^{(1)}$ and the medium with volume V_{m2} and conductivity σ_m. Hence, the effective electrical conductivity of the RVE can be calculated using Eq.(4) as follows,

$$\sigma_e = \frac{2V_{m2}\sigma_m^2+(3V_i^*+V_{m2})\sigma_i^*\sigma_m}{(3V_i^*+2V_{m2})\sigma_m+V_{m2}\sigma_i^*} \tag{15}$$

It is obvious that, in Eq.(15) if $V_{m2}=0$ then $\sigma_e=\sigma_i^*=\sigma_e^{(1)}$. This implies that Eq.(14) can be also applied to Case 2 for calculating the effective electrical conductivity of the RVE.

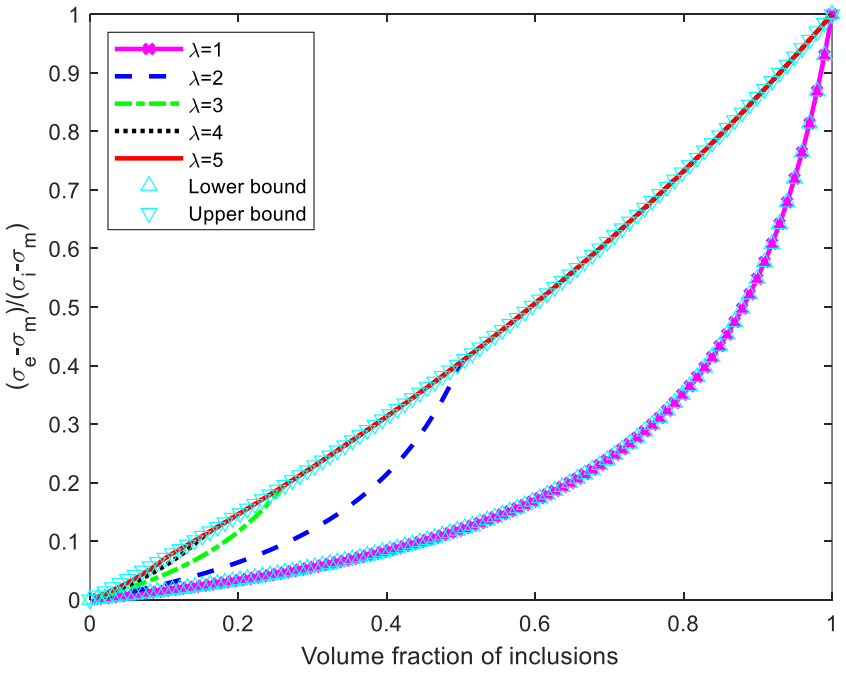

(a)

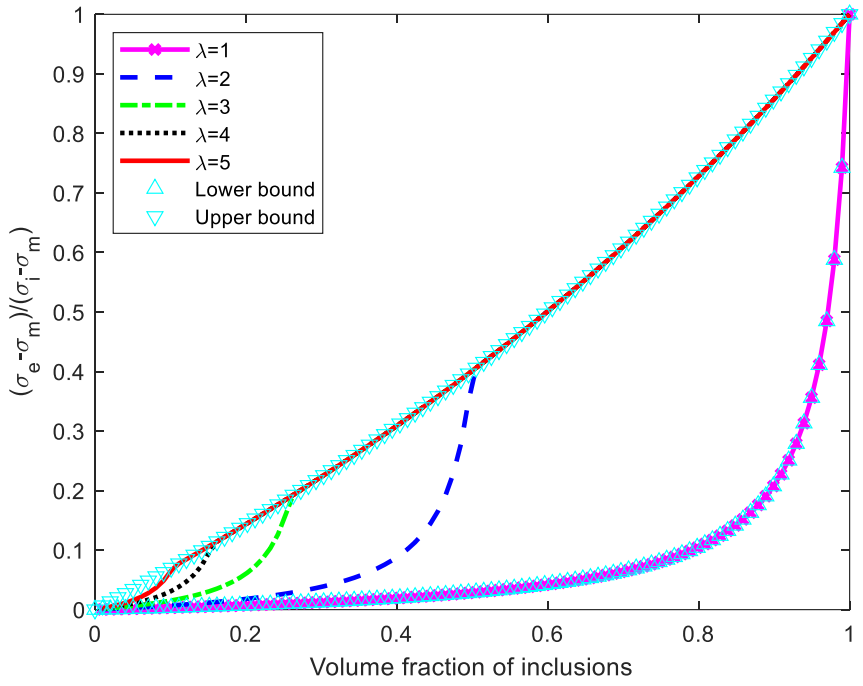

(b)

Figure 4. Variation of effective electrical conductivity of composite with volume fraction of inclusions for different aspect ratios of inclusions. (a) σ_i/σ_m=20 and (b) σ_i/σ_m=100.

For given aspect ratio λ and volume fraction V_i of CNTs, one can calculate a from Eq.(8) first. If the calculated (λa) is less than one then V_{m1} and V_{m2} are calculated using Eqs.(9) and (10). If the calculated (λa) is not less than one then a need be re-calculated by using Eq.(11) and the corresponding V_{m1} and V_{m2} need be calculated using Eqs.(12) and (13). After V_{m1} and V_{m2} are obtained, the effective electrical conductivity of the composite can be calculated using Eqs.(14) and (15).

Fig.4 shows the effect of the aspect ratio on the effective electrical conductivity of the composite material for two cases of σ_i/σ_m=20 and σ_i/σ_m=100, in which the different values of σ_e for different aspect ratios are calculated using Eqs.(14) and (15), whereas the superimposed upper and lower bounds are calculated using Eqs.(4) and (5) of the spherical model, respectively. It can be seen from the figure that the effective conductivity calculated for λ=1 is identical to the lower bound given by the spherical model. This is because when λ=1 the sub-domain shown in Fig.3b is fully occupied by the inclusions (that is V_{m1}=0 and $\sigma_e^{(1)}=\sigma_i$), and in this case the inclusions in the unit volume cube of RVE shown in Fig.3a are always covered by the medium until V_i reaches to 1. The results displayed in Fig.4 for different aspect ratios show that σ_e increases remarkably with increased aspect ratio. However, it is noticed that the aspect ratio-induced increase ceases when the volume fraction of inclusions reaches to a threshold value. For each aspect ratio there is a corresponding threshold volume fraction, after which the curve merges to the upper bound curve given by the spherical model, indicating that

the aspect ratio has no longer effect on the calculated σ_e. The larger the aspect ratio, the smaller the threshold volume fraction. Also, the larger the ratio of σ_i/σ_m, the faster the increase of σ_e from the lower bound to the upper bound.

Physically, the curve of $\sigma_e \sim V_i$ shown in Fig.4 can be divided into two parts according to its threshold volume fraction. Before the volume fraction reaches to its threshold value σ_e is calculated based on the assumption that the inclusions are covered by the medium, and thus the obtained σ_e could be underestimated although $\sigma_e^{(1)}$ in the sub-domain may be overestimated. After the volume fraction reaches to its threshold value σ_e is calculated based on the assumption that the medium is covered by the inclusions, and thus the obtained σ_e could be overestimated. When the volume fraction attends to its threshold value σ_e has a jump from an underestimated value to an overestimated value.

4. Percolation threshold of CNTs-reinforced composites

As described above, the effective electrical conductivity of the composite increases with the volume fraction of inclusions but the rate of increase is different in different volume fraction regions. In particular, there is a critical point before which all randomly distributed inclusions are isolated but after which some of randomly distributed inclusions becomes connective. The volume fraction of inclusions at this critical point is called percolation threshold, which, as demonstrated in Fig.4, depends upon the aspect ratio of inclusions. Percolation is a nonlinear phenomenon. It represents the sudden change in the behaviour of a certain parameter in the multiphase material caused by the volume fraction change of the material. The percolation behaviour becomes pronounced when the mixture consists of components which have a strong contrast in their properties. In literature the mixing formulas predict percolation but the threshold volume fraction is different depending on the mixing rule. For the case of 3-D spherical high-permittivity inclusions, for instance, the percolation threshold is 0.25 given by the Coherent potential formula, 0.33 given by the Polder–van Santen formula, and 1.0 given by the Maxwell Garnett rule [35]. For the composites with inclusions of large aspect ratio, however, their percolation threshold would be much small, as demonstrated in Fig.4.

The threshold volume fraction shown in Fig.4 also reflects the percolation threshold of the composite. According to Eq.(8) and the connective condition $\lambda a=1$ of inclusions, the percolation threshold of the composite thus can be calculated as,

$$V_{i,th} = \frac{3}{\lambda^2} - \frac{2}{\lambda^3} \tag{16}$$

where $V_{i,th}$ is the percolation threshold of the composite or the threshold volume fraction of the inclusions. It is obvious that if $\lambda=1$ then Eq.(16) gives $V_{i,th}=1.0$ which corresponds to the Maxwell Garnett rule. Fig.5 shows the variation of the threshold volume fractions with aspect ratio of inclusions calculated using Eq.(16). It can be seen from the figure that, the threshold volume fraction of inclusions decreases with the increase of aspect ratio and the relationship between them is almost linear in the log-log plot except for the region where λ is close to one. For example, for the composite of inclusions with aspect ratio 20 and 50, the threshold volume fraction of inclusions is about 0.007 and 0.0012, respectively.

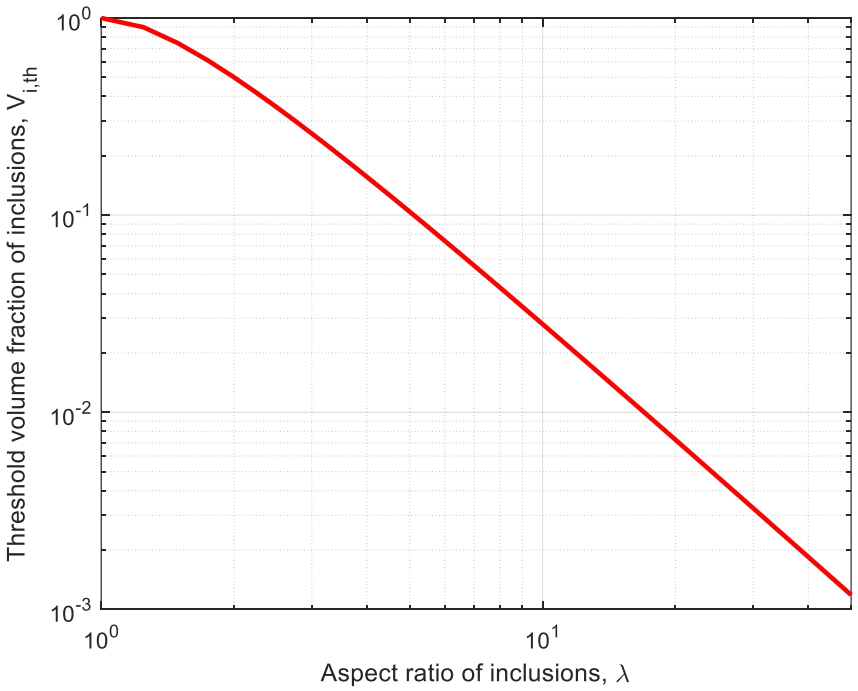

Figure 5. Variation of threshold volume fraction with aspect ratio of inclusions.

5. Calculation of electrical conductivity of CNTs fibre-reinforced composites

As discussed in the previous section, the percolation threshold of a composite can be reduced by increasing the aspect ratio of inclusions in the composite. For the composite whose volume fraction of inclusions is lower than its threshold volume fraction its electrical conductivity is mainly controlled by the lower bound given by the spherical model; whereas for the composite whose volume fraction of inclusions is higher than its threshold volume fraction its electrical conductivity is controlled by both the lower and upper bounds given by the spherical model. In the light of this concept, a simple equation given by Eq.(17) is proposed for calculating the effective electrical conductivity of the composite with considering the effect of aspect ratio of inclusions,

$$\sigma_e = \frac{2V_m\sigma_m^2+(3V_i+V_m)\sigma_i\sigma_m}{(3V_i+2V_m)\sigma_m+V_m\sigma_i}[1-f(V_i)] + \frac{2V_i\sigma_i^2+(3V_m+V_i)\sigma_i\sigma_m}{(3V_m+2V_i)\sigma_i+V_i\sigma_m}f(V_i) \tag{17}$$

where $f(V_i)$ is the weight function, which is defined as follows,

$$f(V_i) = \begin{cases} 0 & V_i \le V_{i,th} \\ \left(\frac{V_i-V_{i,th}}{1-V_{i,th}}\right)^{\alpha} & V_i > V_{i,th} \end{cases} \tag{18}$$

where α is a constant which can be determined using experimental data, but usually α =1 can be used. For most CNTs fibre-reinforced composites $\sigma_i >> \sigma_m$, Eq.(17) thus can be simplified as follows,

$$\sigma_e = \frac{(2V_i+1)\sigma_m}{1-V_i}[1 - f(V_i)] + \frac{2V_i\sigma_i}{3-V_i}f(V_i) \quad (19)$$

Physically, the weight function represents how quick the effective electrical conductivity of the composite jumps from its lower bound to its upper bound. The larger the constant α, the slower the increase of σ_e. The concept of using a weight function is because even the volume fraction of inclusions is greater than its percolation threshold, some of inclusions are still embedded by the medium materials. In other words, not all inclusions are completely percolated and take fully active unless the volume fraction of inclusions reaches to 1. To demonstrate the present model with aspect ratio effect, Fig.6 shows a comparison of the effective electrical conductivities of ethylene-octene-copolymer (EOC) composite containing multi-walled carbon nanotubes (MWCNTs) as the inclusions, predicted using Eqs.(16) and (19) and measured in experiments [36]. To see the effect of σ_i Fig.6 also includes the results of carbon fibres (CFs) reinforced EOC composite. In the prediction the electrical conductivities of MWCNTs, CFs and EOC are taken as σ_i=166 S/m, σ_i=1660 S/m, σ_m=2.5x10^{-7} S/m, respectively, the aspect ratio for both MWCNTs and CFs is taken as λ=7, and the weight function is taken as α=1. It can be seen from the figure that the prediction is in good agreement with the experimental data for both MWCNTs/EOC and CFs/EOC composites, indicating that the present model is logical and appropriate although mathematically it is very simple.

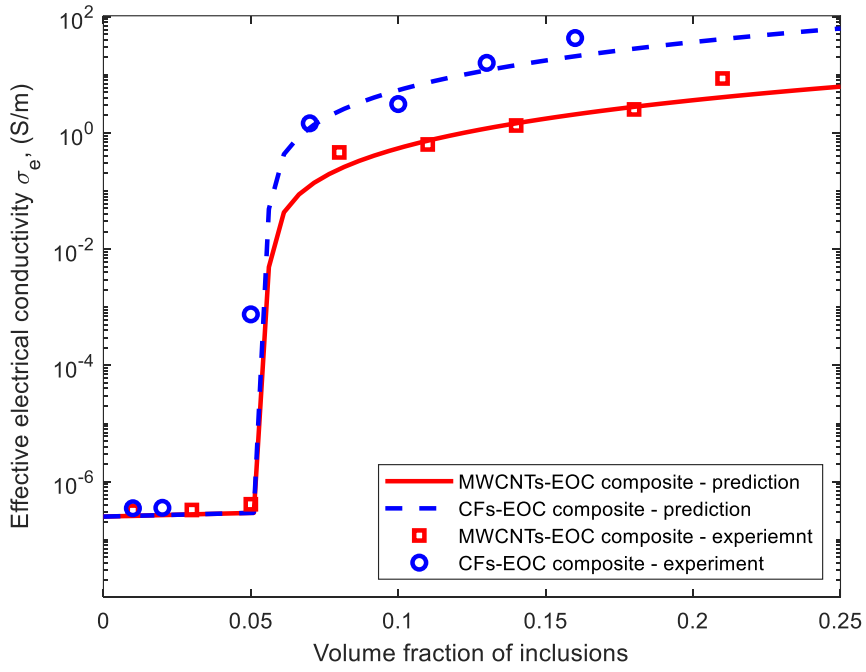

Figure 6. Comparison between analytically predicted and experimentally measured effective electrical conductivities of MWCNTs/EOC and CFs/EOC composites (Parameters used in prediction are MWCNTs σ_i=166 S/m, CFs σ_i=1660 S/m, EOC σ_m=2.5x10^{-7} S/m, λ=7, α=1).

Fig.7 shows another example that is for CNTs-reinforced epoxy composite, in which the predicted effective electrical conductivity is calculated using Eqs.(16) and (19) and the

experimental data were obtained from a published reference [21]. In the experiments the composite was made by using multi-walled CNTs fibres as the inclusions and epoxy resin as the medium. In the prediction the electrical conductivities of CNTs and epoxy are taken as σ_i=500 S/m and σ_m=1.0x10^{-14} S/m, respectively. The weight function uses α=1. The densities of the CNTs and hardened epoxy resin are ρ_i=2250 kg/m^3 and ρ_m=1150 kg/m^3, respectively. The relationship between the volume fraction V_i and mass fractions m_i of CNTs in the composite thus is given as follows,

$$V_i = \frac{m_i \rho_m}{m_i \rho_m + (1-m_i)\rho_i} \tag{20}$$

The CNTs fibres supplied from manufacturers have large aspect ratios (>200). However, after they were mixed with epoxy resin their actual aspect ratio was reduced significantly. This is evident by their SEM image [21], which shows the CNTs become non-straightness and were embraced like wire ball. Thus in the prediction λ=50 is used. It is apparent from the comparison shown in Fig.7 that there is good agreement between the prediction and experimental measurement. This demonstrates that the present model is able to predict the electrical behaviour of the composite made from the two components with huge distinct electrical properties.

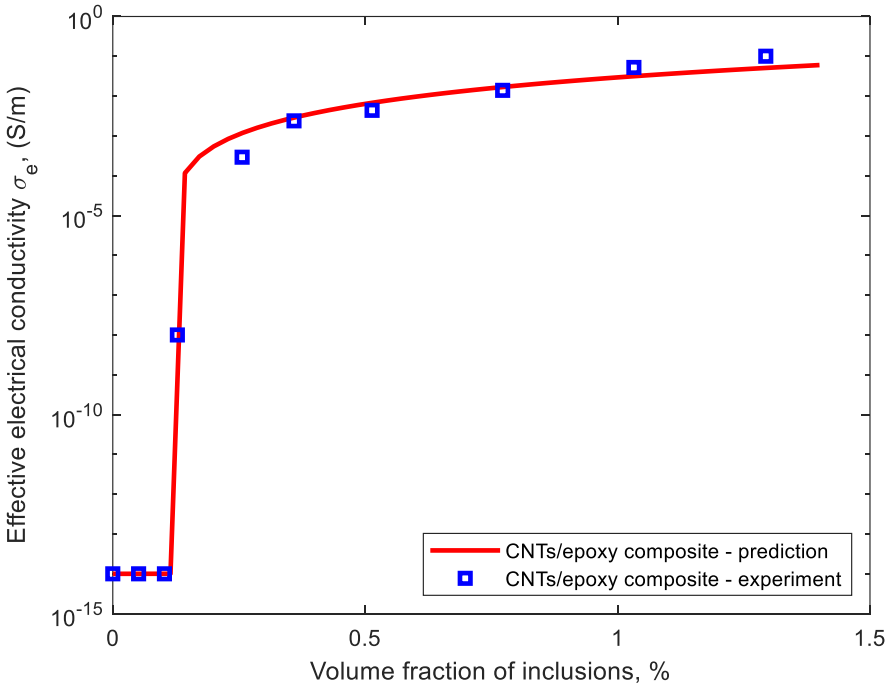

Figure 7. Comparison between predicted and measured effective electrical conductivities of CNTs/epoxy composite (σ_i=500 S/m, σ_m=1.0x10^{-14} S/m, λ=50, α=1).

6. Conclusions

This paper has presented an analytical study on the electrical conductivity of composites containing a homogeneous medium reinforced by randomly distributed discrete inclusions. The study was focussed on the effect of the aspect ratio of inclusions on the percolation threshold of the composites. Analytical expressions for calculating the threshold volume fraction and corresponding effective electrical conductivity of the composite have been derived. The present analytical model has been validated by using experimental data published in literature for CNTs reinforced polymer composites. From the present study the following conclusions can be drawn.

- The aspect ratio of inclusions has a significant influence on the percolation threshold of the composite. The larger the aspect ratio of the inclusions, the smaller the threshold volume fraction of the inclusions.
- For a composite whose inclusion volume fraction is smaller than the threshold volume fraction, the inclusions have a limited effect on the electrical conductivity and the effective electrical conductivity of the composite can be estimated using the lower bound given by the spherical model.
- For a composite whose inclusion volume fraction is greater than the threshold volume fraction, the inclusions have a huge effect on the electrical conductivity and the effective electrical conductivity of the composite can be estimated using the combined lower and upper bounds given by the spherical model.
- For a composite containing high conductive inclusions but low conductive medium its electrical conductivity increases very slowly with increased volume fraction of inclusions until the inclusions reach to a threshold volume fraction. At the threshold volume fraction point the electrical conductivity of the composite has a significant jump, and after then it increases continuously but modestly with the increased inclusion volume fraction.

Acknowledgments - This research was supported by the Korean Agency for Infrastructure Technology Advancement (KAIA) via a grant funded by the Ministry of Land, Infrastructure and Transport (19CTAP-C151808-01) in South Korea.

Declaration of interests - The authors declare that they have no known competing financial interests or personal relationships that could have appeared to influence the work reported in this paper.

References

[1] M. Paradise, T. Goswami, Carbon nanotubes – production and industrial applications. Materials & Design 28(5) (2007) 1477-1489.

[2] C. Li, E.T. Thostenson, T.W. Chou, Sensors and actuators based on carbon nanotubes and their composites: A review. Composites Science and Technology 68(6) (2008) 1227–1249.

[3] N. Hu, H. Fukunaga, S. Atobe, Y. Liu, J. Li, Piezoresistive strain sensors made from carbon nanotubes based polymer nanocomposites. Sensors 11(11) (2011) 10691–10723.
[4] Q.Q. Ni, C.S. Zhang, Y. Fu, G. Dai, T. Kimura, Shape memory effect and mechanical properties of carbon nanotube/shape memory polymer nanocomposites. Composite Structures 81(2) (2007) 176-184.
[5] G.T. Pham, Y.Bin Park, Z. Liang, C. Zhang, B. Wang, Processing and modeling of conductive thermoplastic/carbon nanotube films for strain sensing. Composites Part B: Engineering 39(1) (2008) 209-216.
[6] J.N. Dastgerdi, G. Marquis, M. Salimi, The effect of nanotubes waviness on mechanical properties of CNT/SMP composites. Composites Science and Technology 86 (2013) 164-169.
[7] H. Lu, Y. Yao, W.M. Huang, J. Leng, D. Hui, Significantly improving infrared light-induced shape recovery behavior of shape memory polymeric nanocomposite via a synergistic effect of carbon nanotube and boron nitride. Composites Part B: Engineering 62 (2014) 256-261.
[8] M.H. Jomaa, K. Masenelli-Varlot, L. Seveyrat, L. Lebrun, M.C.D. Jawhar, E. Beyou, J.Y. Cavaillé, Investigation of elastic, electrical and electromechanical properties of polyurethane/grafted carbon nanotubes nanocomposites. Composites Science and Technology 121 (2015) 1-8.
[9] A.G. Arani, M. Jamali, M. Mosayyebi, R. Kolahchi, Wave propagation in FG-CNT-reinforced piezoelectric composite micro plates using viscoelastic quasi-3D sinusoidal shear deformation theory. Composites Part B: Engineering 95 (2016) 209-224.
[10] R. Kolahchi, M.S. Zarei, M.H. Hajmohammad, A. Nouri, Wave propagation of embedded viscoelastic FG-CNT-reinforced sandwich plates integrated with sensor and actuator based on refined zigzag theory. International Journal of Mechanical Sciences 130 (2017) 534-545.
[11] M.K.H. Aghdam, R. Ansari, Thermal conductivity of shape memory polymer nanocomposites containing carbon nanotubes: a micromechanical approach. Composites Part B: Engineering 162 (2019) 167-177.
[12] X. Xia, J. Hao, Y. Wang, Z. Zhong, G.J. Weng, Theory of electrical conductivity and dielectric permittivity of highly aligned graphene-based nanocomposites. Journal of Physics: Condensed Matter 29(20) (2017) 205702.
[13] C. Fang, J. Zhang, X. Chen, G.J. Weng, Calculating the electrical conductivity of graphene nanoplatelet polymer composites by a Monte Carlo method. Nanomaterials 10(6) (2020) E1129.
[14] P. Spanos, P. Elsbernd, B. Ward, T. Koenck, Estimation of the physical properties of nanocomposites by finite-element discretization and Monte Carlo simulation. Phil. Trans. R. Soc. A. 371(1993) (2013) 20120494.
[15] F. Liu, Y. Sun, W. Sun, Z. Sun, J.T.W. Yeow, Numerical and experimental study of radiation induced conductivity change of carbon nanotube filled polymers. Nanotechnology 28(25) (2017) 255501.
[16] D.A.G. Bruggeman, Berechnung verschiedener physikalischer Konstanten von heterogenen Substanzen. Ann. Phys. (Leipzig) 416(7) (1935) 636-664.

[17] D.S. McLachlan, An equation for conductivity of binary mixtures with anisotropic grain structures. J Phys C: Solid State Phys. 20(7) (1987) 865-877.
[18] D.S. McLachlan, M. Blaszkiewicz, R.E. Newnham, Electrical resistivity of composites. J Am Ceram Soc. 73(8) (1990) 2187-2203.
[19] F. Lux, Review: models proposed to explain the electrical conductivity of mixtures made of conductive and insulating materials. J Mater Sci 28(2) (1993) 285-301.
[20] M. Sahini, M. Sahimi, Application of Percolation Theory. CRC Press, London (1994).
[21] S.H. Jang, L.Y. Li, Self-sensing carbon nanotube composites exposed to glass transition temperature. Materials 13 (2020) 259.
[22] J. Bigalke, Investigation of the conductivity of random networks. Physica A 272(3-4) (1999) 281–293.
[23] N.F. Uvarov, Estimation of electrical properties of composite solid electrolytes of different morphologies. Solid State Ionics 302 (2017) 19-24.
[24] A. Giraud, I. Sevostianov, V.I. Kushch, P. Cosenza, D. Prêt, J.F. Barthélémy, A. Trofimov, Effective electrical conductivity of transversely isotropic rocks with arbitrarily oriented ellipsoidal inclusions. Mechanics of Materials 133 (2019) 174-192.
[25] A. Carrillo, I.R. Martı´n-Domı´nguez, A. Rosas, A. Ma´rquez, Numerical method to evaluate the influence of organic solvent absorption on the conductivity of polymeric composites. Polymer 43(23) (2002) 6307–6313.
[26] S. Kanaun, Calculation of electro and thermo static fields in matrix composite materials of regular or random microstructures. International Journal of Engineering Science 49(1) (2011) 41-60.
[27] Q.F. Liu, D. Easterbrook, L.Y. Li, D.W. Li, Prediction of chloride diffusion coefficients in concrete using meso-scale multi-phase transport models. Magazine of Concrete Research 69(3) (2017) 134-144.
[28] E. Herve, Thermal and thermoelastic behaviour of multiply coated inclusion-reinforced composites. International Journal of Solids and Structures 39(4) (2002) 1041-1058.
[29] E. Herve, A. Zaoui, Elasticity behaviour of multiply coated fibre-reinforced composites. International Journal of Engineering Science 33(10) (1995) 1419-1433.
[30] L.Y Li, J. Xia, S.S Lin, A multi-phase model for predicting the effective diffusion coefficient of chlorides in concrete. Construction and Build Materials 26(1) (2012) 295-301.
[31] A. Bouhamed, A. Al-Hamry, C. Müller, S. Choura, O. Kanoun, Assessing the electrical behaviour of MWCNTs/epoxy nanocomposite for strain sensing. Composites Part B: Engineering 128 (2017) 91–99.
[32] J. Shen, S. Buschhorn, J.T.M. de Hosson, K. Schulte, B. Fiedler, Pressure and temperature induced electrical resistance change in nano-carbon/epoxy composites. Composites Science and Technology 115 (2015) 1–8.
[33] N.T. Dinh, O. Kanoun, Temperature-compensated force/pressure sensor based on multi-walled carbon nanotube epoxy composites. Sensors 15 (2015) 11133–11150.
[34] S.H. Jang, H.M. Yin, Effective electrical conductivity of carbon nanotube-polymer composites: A simplified model and its validation. Materials Research Express 2 (2015) 045602.

[35] A. Sihvola, S. Saastamoinen, K. Heiska, Mixing rules and percolation. Remote Sensing Reviews 9(1-2) (1994) 39–50.
[36] Z. Sedláková, G. Clarizia, P. Bernardo, J.C. Jansen, P. Slobodian, P. Svoboda, M. Kárászová, K. Friess, P.I. Izak, Carbon nanotube- and carbon fiber-reinforcement of ethylene-octene copolymer membranes for gas and vapor separation. Membranes 4(1) (2014) 20-39.